Journal Homepage: -www.journalijar.com

INTERNATIONAL JOURNAL OF ADVANCED RESEARCH (IJAR)

Article DOI:10.21474/IJAR01/18020
DOI URL: http://dx.doi.org/10.21474/IJAR01/18020

RESEARCH ARTICLE

SYNTHESIS AND STUDY ON THE PROPERTIES OF $CaMoO_4:Eu^{3+}$ CO–DOPEDTb^{3+} MATERIALS TO ENHANCED RED PHOTOLUMINESCENCE

Nhuong Chu Manh[1], Mai An Pham[2] and Huan Pham Van[3]

1. Faculty of Chemistry, Thai Nguyen University of Education, Thai Nguyen City 250000, Vietnam.
2. Faculty of Physics, Thai Nguyen University of Education, Thai Nguyen City 250000, Vietnam.
3. Faculty of Natural Sciences, Electric, Electric Power University, Hanoi City 100000, Vietnam.

Manuscript Info

Manuscript History
Received: 15 October 2023
Final Accepted: 18 November 2023
Published: December 2023

Key words:-
$Ca_{0.99-y}Tb_{0.01}MoO_4:yEu^{3+}$, Nanophosphors, Red, Lifetime

Abstract

$Ca_{0.99-y}Tb_{0.01}MoO_4:yEu^{3+}$nanophosphors weresuccessfullysynthesizedbyhydrothermal method. All the samples can be excited by 395nm wavelengths for generation of red color emission. Enhancement in $^5D_0\rightarrow{}^7F_2$ (616 nm) emission (f–f transition) of Eu^{3+}ionis observed when Tb^{3+}ionis co–doped in $CaMoO_4:Eu^{3+}$. This is due to the efficient energy transfer from Tb^{3+} to Eu^{3+} ions. Introduction of Tb^{3+} in the system does not lead to the change of emission wavelength of Eu^{3+}. However, $Tb^{3+}$and Eu^{3+}co–doped in the system induces a shift in Mo-O charge transfer band absorption from 262nm to (413–431 nm). This may be due to the increase in electronegativity between Mo and O bond in the presence of Eu^{3+}andTb^{3+}leading to change in crystal field environment of Mo^{6+} in MoO_4^{2-}. At the optimal concentration of Eu^{3+}, an enhancement in emission by a factor of ~5.6 in the respective excitation at 616nm ($^5D_0\rightarrow{}^7F_2$) is observed. The chromaticity coordinates (CIE) of all $Ca_{0.99-y}Tb_{0.01}MoO_4:yEu^{3+}$ nanophosphors are in the red region. The luminescence lifetime values are0.812 ms to 1.20 ms. The energy transfer is observed to occur mainly via dipole–dipole interactions.

Introduction:-

Nowaday, the luminescence of rare earth ions(RE^{3+})has attractedintensive investigations due to the abundant emission spectra caused bytheir special 4f electronic configuration. Phosphors are an important part of whitelight LEDs, which require a long life, high color rendering index (CRI), high luminosity efficiency, color neutrality, poor thermal stability, and their emission diminishes over time and environmental friendly characteristics. The above requirements can be improved by RE^{3+}doped luminescent materials due to 4f–4f transition in rare earths [1–5]. Ion Eu^{3+} (1.066 Å) and Tb^{3+} (1.027 Å) co–doped compounds have been paid considerable attention due to the strong red emission ($^5D_0\rightarrow{}^7F_2$transition of Eu^{3+}, 616 nm) and the green emission at 545 nm($^5D_4\rightarrow{}^7F_5$) and the blue emission at 489 nm ($^5D_4\rightarrow{}^7F_6$), which are due to internal 4f–4f electron transitions of Tb^{3+}. The $CaMoO_4:RE^{3+}$material with scheelite structure has strong 4f–4f transitional absorption and emission due to the effect of polarization of MoO_4^{2-}. As well known, the luminescence properties of RE^{3+} doped materials may be strongly influenced by the crystal field environmentaround the RE ions in the host. Thus, it is important to choose an appropriate host material. $CaMoO_4$ belongs to the scheelitestructure, which is assembled by CaO_8 dodecahedra and MoO_4 tetrahedron. In addition, $CaMoO_4$ has good chemical and heat stability. Therefore, $CaMoO_4$ is considered to be an excellent matrix material for luminescence [6–11, 13].

Corresponding Author:- Nhuong Chu Manh
Address:- Faculty of Chemistry, Thai Nguyen University of Education, Thai Nguyen City 250000, Vietnam.

Khanna et al [1] synthesized phosphor crystals of calcium molybdate doped with dopant Eu^{3+}, Dy^{3+}, Tb^{3+} grown using flux growth method have been shown to exhibit higher excitation efficiency than the powders synthesized by solid state reaction process at a temperature around 1100 ^{o}C. Using the excitation wavelengths of 465 nm, 454 nm and 489 nm for $CaMoO_4:Eu^{3+}$, $CaMoO_4:Dy^{3+}$ and $CaMoO_4:Tb^{3+}$, respectively, intense emission lines at 615 nm ($^5D_0$-$^7F_2$ transition of Eu^{3+}), 575 nm ($^4F_{9/2}$-$^6H_{13/2}$ of Dy^{3+}) and 550 nm ($^5D_4$-$^7F_5$ of Tb^{3+}) were observed. The optimized doping concentrations of 12%, 2% and 5% for Eu^{3+}, Dy^{3+} and Tb^{3+}, respectively, provided the highest luminescence intensity. These phosphors could potentially be used for the fabrication of phosphor-converted light emitting diodes (pc–LEDs).

Akta Verm et al [2] have successfully developed $CaMoO_4:RE^{3+}$ (RE = Tb, Sm, Tm, Er, Yb) phosphors as a spectral converter for solar cell application by using hydrothermal method. The XRD pattern contains prominent peaks located at 28.74^{o}, 47.08^{o}, 58.03^{o}, 76.11^{o} corresponds to (112), (204), (312) and (316)planes, respectively. The crystallite size was found in the range of 10–60 nm. The calculated values of band gap for $CaMoO_4:Tb^{3+}/Sm^{3+}/Tm^{3+}$ and (1%)Er^{3+}, (2%)Yb^{3+} dopedand co–doped $CaMoO_4$ phosphors were found 3.88 eV, 3.85 eV, 3.82 e and 3.76 eV, respectively. The as synthesized $CaMoO_4:Tb^{3+}$, Sm^{3+}, Tm^{3+} downshifting (DS) phosphors exhibit hypersensitive green, red and blue emission at 547 nm, 600 nm and 453 nm corresponding to $^5D_4\rightarrow{}^7F_5$, $^4G_{5/2}\rightarrow{}^6H_{7/2}and^1D_2\rightarrow{}^3F_4$ transitions, respectively. The spectrum of $CaMoO_4:Tb^{3+}$ phosphor consists of a prominent peak at 378 nm arises due to f–f transition of Tb^{3+} ions from ground state $^7F_6$ to $^5D_3$ level. The spectrum contains various peaks at 488 nm, 547 nm, 585 nm, 620 nm due to $^5D_4\rightarrow{}^7F_6$, $^5D_4\rightarrow{}^7F_5$, $^5D_4\rightarrow{}^7F_4$, $^5D_4\rightarrow{}^7F_3$ transitions, respectively.

Anees A. Ansari et al [3]synthesized $CaMoO_4$:Tb, $CaMoO_4$:Tb@$CaMoO_4$and$CaMoO_4$:Tb@$CaMoO_4$@SiO_2coreeshell nanoparticles have been successfully prepared by polyol process with urea thermal decomposition. The XRD results indicate that the obtained $CaMoO_4$:Tb is sheelite tetragonal structure and well crystallized at 150 ^{o}C. The average crystallite size of the synthesized nanoparticles is calculated using the Scherrer formula for the major (112) reflection plane observed at ~28.8^{o}about 21.1, 32.4 and 48.2 nm, respectively. The absorption spectra of $CaMoO_4$:Tb nanoparticles reveals two well resolved broad absorption bands at 206 nm (6.0 eV) and 234 nm (5.3 eV). The emission spectra recorded at room temperature in the spectral range of 400–700 nm with excitation at 325 nm (3.82 eV) displayed several well–known emission bands corresponding to the intra 4f transitions $^5D_4\rightarrow{}^7F_n$ (n = 0–6), which belong to the characteristic transition of Tb^{3+} ion. These emission spectra reveal six emission transitions in the visible region which are observed at 488 nm (2.54 eV; $^5D_4$-$^7F_6$), 545 nm (2.27 eV; $^5D_4$-$^7F_5$), 586 nm (2.12 eV; $^5D_4$-$^7F_4$), 620 nm (2.00 eV; $^5D_4$-$^7F_3$), 641–658 nm (1.90 eV; $^5D_4$-$^7F_2$) and 680 nm (1.82 eV; $^5D_4$-$^7F_0$), with the hypersensitive $^5D_4$-$^7F_5$ transition as the most prominent one, and hence can provide information about the chemical environment of the Tb^{3+} ion. The comparative emission spectra show that the peak positions of Tb^{3+} ions are not affected or destroy the structure and luminescence properties of $CaMoO_4:Tb^{3+}$ phosphor after covered the $CaMoO_4$ and SiO_2 nano–layers around the $CaMoO_4:Tb^{3+}$ nanocrystals, could be due to no alteration of symmetry of the core lattice. The highest phosphorescence intensity is observed for $CaMoO_4$:Tb regardless of $CaMoO_4$ and SiO_2 layer coated coreeshell nanoparticles, most probably by the UV light absorption and scattering of $CaMoO_4$ and amorphous SiO_2 that reduces the excitation irradiation intensity.

Yongqing Zhai et al [4] synthesized a series of Dy^{3+}/Eu^{3+} co–doped $CaMoO_4$ phosphors by a facile microwave radiation synthesis method. The the band gap energy (E_g) of $Ca_{0.98}MoO_4:0.02Dy^{3+}$ and $Ca_{0.978}MoO_4:0.02Dy^{3+},0.002Eu^{3+}$ is estimated to be 3.68 eV and 3.64 eV, respectively. The SEM of two samples, show the average size of the fine spherical–like grains is about 0.29 and 0.38 μm, respectively. The emission spectra of phosphors under the excitation of 301 nm, contain a broad band ranging from 400 to 550 nm and a narrow peak located at 573 nm. The broad band belongs to the emission of internal MoO_4^{2-} and the $^4F_{9/2}\rightarrow{}^6H_{15/2}$ magnetic dipole transition of Dy^{3+} (484 nm). The peak at 573 nm is attributed to the $^4F_{9/2}\rightarrow{}^6H_{13/2}$ electric dipole transition of Dy^{3+}. Besides, for $Ca_{0.978}MoO_4:0.02Dy^{3+},0.002Eu^{3+}$ phosphor, the characteristic emissions of Eu^{3+} can be observed, which are corresponding to the $^5D_0\rightarrow{}^7F_1$ (589 nm), $^5D_0\rightarrow{}^7F_2$ (613 nm) and $^5D_0\rightarrow{}^7F_3$ (652 nm) transitions, respectively. The chromaticity coordinates (CIE) of $Ca_{0.98-x}MoO_4:0.02Dy^{3+},xEu^{3+}$ (x = 0–0.008) phosphors under the excitation at 254 nm, were measured (0.3139, 0.4895) to (0.6238, 0.3658) and CCT values of (1198–5956 K). The average decay time of Dy^{3+} is determined to be 20.33, 19.49, 17.90, 17.57 and 15.87 μs, respectively. The energy transfer efficiency (η_{ET})from Dy^{3+} to Eu^{3+}, is determined to be 4.1%, 11.9%, 13.5% and 21.9%, corresponding to x = 0.002–0.008 in $Ca_{0.98-x}MoO_4:0.02Dy^{3+},xEu^{3+}$, respectively. The energy transfer mechanism of $Dy^{3+}\rightarrow Eu^{3+}$ is the dipole-dipole interaction. The samples can emit multiple colors of yellow–green, yellow, orange–reddish and red by adjusting Eu^{3+} doping content. Under 301 nm excitation, the increase of Eu^{3+} content in $CaMoO_4:Dy^{3+},Eu^{3+}$ led to

the enhancement of red emission (613 nm) of Eu^{3+} and the decrease of blue and yellow emissions of Dy^{3+}, which was possibly due to the efficient energy transfer (ET) from level of Dy^{3+} to $^5D_0$ level of Eu^{3+} through the phonon–aided non–radiative relaxation. The phosphors could generate different color light from yellow–green through yellow and orange–reddish and eventually to red by properly tuning the content of Eu^{3+} based on the ET process, which suggested that they might be potentially applied in the fields of lighting and display.

Shidong Li et al [5] successfully synthesized $CaMoO_4$:5%Tb^{3+},x%Eu^{3+}(x = 0.3, 0.5, 1.0, 2.0) phosphors by precipitation method. The room temperature PLE spectrum of the $CaMoO_4$:5%Tb^{3+}sample monitoring at 545.5 nm and 486 nm, corresponding to $^5D_4\rightarrow{}^7F_5$ and $^5D_4\rightarrow{}^7F_6$transitions of Tb^{3+}. The $CaMoO_4$:1%Eu^{3+}PLE spectrum are 395 nm and 465 nm for $^7F_0\rightarrow{}^5L_6$ and $^7F_0\rightarrow{}^5D_2$ of Eu^{3+} as the monitoring wavelength is 616 nm. The PLE spectrum of $CaMoO_4$:5%Tb^{3+},0.3%Eu^{3+}, monitoring at 616 nm transition from Eu^{3+} ($^5D_0\rightarrow{}^7F_2$). The excitation peaks are from Eu^{3+} or Tb^{3+} different energy level transitions for Eu^{3+} at 362 nm ($^7F_0\rightarrow{}^5D_4$), 381 nm ($^7F_0\rightarrow{}^5L_7$), 395 nm ($^7F_0\rightarrow{}^5L_6$), 416 nm ($^7F_0\rightarrow{}^5D_3$), 465 nm ($^7F_0\rightarrow{}^5D_2$), and at 486 nm ($^7F_6\rightarrow{}^5D_4$) for Tb^{3+}. The room temperature photoluminescence (PL) spectra excited by 270 nm of $CaMoO_4$:5%Tb^{3+}, $CaMoO_4$:5%Tb^{3+},0.3%Eu^{3+}, and $CaMoO_4$:1%Eu^{3+} phosphors, show the 4f–4f transition of Tb^{3+} locating at 489 nm ($^5D_4\rightarrow{}^7F_6$), 545 nm ($^5D_4\rightarrow{}^7F_5$), 587 nm ($^5D_4\rightarrow{}^7F_4$), and 621 nm ($^5D_4\rightarrow{}^7F_3$), of Eu^{3+} ion's 4f–4f transition at 592 nm ($^5D_0\rightarrow{}^7F_1$), 616 nm ($^5D_0\rightarrow{}^7F_2$), 655 nm ($^5D_0\rightarrow{}^7F_3$), and 702 nm ($^5D_0\rightarrow{}^7F_4$). The fluorescence intensity ratio (FIR) of Eu^{3+} to Tb^{3+} is dependent on temperature, and the FIR increases with the increase of temperature. When FIR of Eu^{3+} to Tb^{3+} is used to characterize the temperature, the sensitivity increases with the increase of Eu^{3+} concentration.

Hyun–Woo Lee et al [6] developed a new method for preparing transparent suspensions of $CaMoO_4$:(1-x)Eu^{3+},(x)Tb^{3+} (x = 0–1) nanophosphors by reacting Ca–oleate (with Eu–oleate and/or Tb–oleate) complexes in hexane with an aqueous $(NH_4)_6Mo_7O_{24}$ solution via a solvothermal reaction in a hexane–water bilayer system. The TEM revealed slightly elongated spherical particles with a mean length and width of 9.5±3.6 and 4.1±1.2 nm, respectively. The photoluminescence emission spectra of the $CaMoO_4$:Eu^{3+} and $CaMoO_4$:Tb^{3+} nanophosphors exhibited intense peaks in the red (614 nm) and green (545 nm) regions, respectively. These emissions originated from the $^5D_0\rightarrow{}^7F_2$ transition of the Eu^{3+} ion and the $^5D_4\rightarrow{}^7F_5$ transition of the Tb^{3+} ion in the $CaMoO_4$ host, respectively. The emission colors in the green–red spectral region could be finely tuned by adjusting the molar fraction of Tb^{3+} ions in the $CaMoO_4$:(1-x)Eu^{3+},(x)Tb^{3+}nanophosphors. The PL emission spectrum of the $CaMoO_4$:Eu^{3+} nanophosphor exhibits a series of emission lines in the range of 550–750 nm due to the $^5D_0\rightarrow{}^7F_J$ (j = 1–4) transitions of Eu^{3+}. Thus, the $CaMoO_4$:Eu^{3+} nanophosphor is a red emitting material, as evident from its strongest emission peak appearing at 614 nm, which is assigned to the $^5D_0\rightarrow{}^7F_2$ transition of Eu^{3+}. Similarly, the PL excitation spectrum of the $CaMoO_4$:Tb^{3+} nanophosphor exhibits a broad CT band at approximately 300 nm, while the PL emission spectrum of the $CaMoO_4$:Tb^{3+} nanophosphor exhibits sharp emission peaks at 489, 545, 587, and 621 nm that originate from the $^5D_4\rightarrow{}^7F_j$ (j = 6, 5, 4, 3) transitions of Tb^{3+}, respectively. Thus, the $CaMoO_4$:Tb^{3+} nanophosphor is a green–emitting material with the most intense emission peak appearing at 545 nm. The characteristic strong peaks at 614 and 545 nm correspond to the $^5D_0\rightarrow{}^7F_2$ transition of Eu^{3+} and the $^5D_4\rightarrow{}^7F_5$ transition of Tb^{3+}, respectively. With an increase in x value, the emission intensities at 614 and 545 nm simultaneously decreased and increased, respectively. The ratio of the emission intensity at 545 nm to the sum of the intensities at 545 and 614 nm increased with increasing x value for the $CaMoO_4$:(1-x)Eu^{3+},(x)Tb^{3+} nanophosphors. Thus, the emission color can be finely tuned from red to green by adjusting the fractions of Tb^{3+} and Eu^{3+} activator ions in the $CaMoO_4$:(1-x)Eu^{3+},(x)Tb^{3+}nanophosphors. This shows that the emission color of the $CaMoO_4$:(1-x)Eu^{3+},(x)Tb^{3+} nanophosphor is tunable. With an increase in x value, the chromaticity coordinates changed from (0.65, 0.34) for the red–emitting $CaMoO_4$:Eu^{3+} nanophosphor to (0.31, 0.60) for the green–emitting $CaMoO_4$:Tb^{3+}. The prepared $CaMoO_4$:(1-x)Eu^{3+},(x)Tb^{3+} suspensions can be used in transparent displays as light emitting materials with tunable emission from red to green region.

R. L. Tranquilinet al [7] successfully synthetized $CaMoO_4$:xRE^{3+} (RE = Eu, Tb, Tm and x = 1, 2, 4 mol%) compounds by one–pot ultrasonic spray pyrolysis method. The values of E_g were within the range of 3.84–3.93 eV. The PL spectra of the $CaMoO_4$:RE^{3+} phosphors exhibited characteristics of each doped ion (Eu^{3+}, Tb^{3+}, Tm^{3+}) emission. Under the excitation of 350 nm, the $^5D_4\rightarrow{}^7F_6$(492 nm) and $^5D_4\rightarrow{}^7F_5$(548 nm) transitions, respectively, which are associated with the emission of Tb^{3+}. This is related to the charge transfer (CT) process from the $[TbO_8]$ to the $[MoO_4]^{2-}$ tetragonal clusters, which corresponds to the 4f→5d transitions. The emission peak at 800 nm is attributed to Tm^{3+}, which is associated with the $^3H_4\rightarrow{}^3H_6$ transition. With respect to Eu^{3+}, $^5D_0\rightarrow{}^7F_j$ (j = 1–4) transitions occurred at the respective wavelengths of 596, 614, 661, and 704 nm. The most intense emission band, $^5D_0\rightarrow{}^7F_2$, of Eu^{3+} is known to have an electric dipole, and this type of transition is highly sensitive to the changes

that occur around the Eu^{3+} cations. The samples with 2 and 4% of RE^{3+} released white emission according to the chromaticity coordinates (0.34, 0.34) and (0.34, 0.33), respectively.

Xiong Jianhui et al [8] synthesized $CaMoO_4:Tb^{3+},Eu^{3+}$ phosphors by precipitation method. By adjusting the co–doped concentration of Eu^{3+} ion in $CaMoO_4:Tb^{3+},Eu^{3+}$ phosphors, can be easily adjusted the emission color of phosphors from green to red. The particle size is uniformly distributed about 1 μm. The emission spectra of $CaMoO_4:x\%Tb^{3+}$ (x = 2–8) phosphors and the excitation wavelength is 486 nm. The concentration quenching of Tb^{3+} ($^5D_4\rightarrow{}^7F_5$) transition green luminescence of $CaMoO_4$ samples which is excited by 486 nm. With the increase of Tb^{3+} concentration, the luminescent intensity of 545.5 nm of Tb^{3+}($^5D_4\rightarrow{}^7F_5$) first increases and then decreases. The best concentration of Tb^{3+} is 5%. When the Tb^{3+} concentration is more than 5%, the luminescent intensity remarkably decreases. This phenomenon is due to the energy transfer between Tb^{3+} ions leading to the concentration quenching. The luminescent properties and the energy transfer mechanism from Tb^{3+} to Eu^{3+} in the phosphors were studied. With the increase of Eu^{3+} concentration, the luminescent colors could be changed from green to red easily because of different proportions of Tb^{3+} and Eu^{3+}.The phosphors had potential application in the anti–counterfeiting technology. With Tb^{3+} doped in the phosphors, the red luminescence of Eu^{3+} by near UV excitation was significantly enhanced. The study also indicated that the energy transfer rate and energy transfer efficiency from Tb^{3+} to Eu^{3+} were increased with the increase of Eu^{3+} concentration, and the energy transfer type between Tb^{3+} and Eu^{3+} was electric dipole-dipole interaction.

Jiaming Deng et al [9] synthesized Tb^{3+}, Eu^{3+} single–doped and co–doped $Ca_2Al_2SiO_7$ (CAS) phosphors by sol–gelmethod. $CAS:Tb^{3+},Eu^{3+}$ phosphors demonstrate tunable luminescence under 238 nm excitation, in which the luminescence color gradually changes from purple–red to cool white, and then to warm white by continuously increasing the concentration of Tb^{3+} ions. The photoluminescence emission spectra for $CAS:0.04Tb^{3+}$ sample excited under 238 nm shows the emission bands at 380–460 nm and 480–650nm, which are ascribed to the $^5D_3\rightarrow{}^7F_J$ (J = 6, 5, 4, 3) and $^5D_4\rightarrow{}^7F_J$ (J = 6, 5, 4, 3) transitions of Tb^{3+} ions. The excitation spectra for $CAS:0.07Eu^{3+}$ sample monitored at 623 nm shows the strongest excitation wavelength at 395 nm. Then the phosphor excites with 395 nm and the maximum emission wavelength is observed at 623 nm, which isascribing to the ^5D-$^7F_2$ transition of Eu^{3+} ions. The emission spectra of $CAS:0.04Tb^{3+}$ and the excitation spectrum of $CAS:0.07Eu^{3+}$ is overlapped in the range of 371–401 nm, indicating that there may exist an ET process of $Tb^{3+}\rightarrow Eu^{3+}$ in $Ca_2Al_2SiO_7$host. Since 350 nm can only excite Tb^{3+} but not Eu^{3+}, the excitation wavelength of 350 nm is selected for investigation the energy transfers from Tb^{3+} to Eu^{3+}. Under 350 nm excitation, the $CAS:0.07Eu^{3+}$ exhibits almost no emission peak at 623 nm. However, the luminescence intensity of Eu^{3+} at 623 nm enhances gradually with increasing the doped ratio of Tb^{3+} ions for the $CAS:xTb^{3+},0.07Eu^{3+}$ samples. To clearly, the intensity of the emission peaks of Tb^{3+} at 549 nm and Eu^{3+} at 623 nm as a function of Tb^{3+} content. It can be seen that the emission intensity of Tb^{3+} at 549 nm increases with the Tb^{3+} doped content and then decreases due to the concentration quenching near x = 0.11, while the emission intensity of Eu^{3+} at 623 nm shows a similar variation trends as Tb^{3+} ion. Thus, $Tb^{3+}\rightarrow Eu^{3+}$ ET occurs in the CAS matrix, which enhances the red emission of Eu^{3+} ions. The fluorescence lifetimes determinated are 1.17 ms, 1.25 ms, 1.66 ms, 1.71 ms, 2.26 ms, for x = 0.01, 0.03, 0.07, 0.09, 0.11, respectively. Therefore, the lifetime of Eu^{3+} gradually increases with increasing Tb^{3+} concentration for a fixed Eu^{3+} concentration, which further indicates the existence of energy transfer from Tb^{3+} to Eu^{3+}. The elongation of the fluorescence lifetime of Eu^{3+} with increasing Tb^{3+} ions content further confirms the energy transfer of $Tb^{3+}\rightarrow Eu^{3+}$. The thermal behavior of $CAS:Tb^{3+}$, Eu^{3+} phosphors shows enhanced luminescence intensity for 404 nm emission while suppressed luminescence intensity for 616 nm emissions withraising temperature, implying its potential in optical temperature sensing.

In previous work [10], we successfully synthesized luminescent nanomaterial $CaMoO_4:(0\text{-}7\%)Eu^{3+}$ using hydrothermal method. The materials exist in crystalline formscheelite–type tetragonal structure with $I4_1/a$, with an average diameter according to the Scherrer method of about 26–41 nm. Photoluminescence spectra of $CaMoO_4:Eu^{3+}$ nanophosphors show emission peak at 613–616 nm ($^5D_0\rightarrow{}^7F_2$). The Judd–Ofelt parameters Ω_2 and Ω_4 have been calculated from the photoluminescence emission spectra of $CaMoO_4:5\%Eu^{3+}$, in temperature range 293 K–693 K. Judd–Ofelt intensity parameters uniformly decrease with increasing temperature. The Judd–Ofelt parameters radiative lifetimes and emission cross–sections were calculated. The results indicate that the Eu^{3+} doped $CaMoO_4$ nanophosphors are expected to have applications in the field of solid state lighting and other optical instruments.

In this study, we present the material's characteristics and photoluminescence properties of nano $CaMoO_4$ co–doped europium (III) and tecbium (III) ions, for the purpose of comparing and showing the effect of 1 mol% Tb^{3+} ion on the photoluminescent properties of $CaMoO_4:(1\text{–}10\%)Eu$ (CME) materials [10]. The powder X–Ray diffraction,

Raman scattering, FE–SEMand TEM, EDS, UV–Vis–Drs, the photoluminescence excition, the photoluminescence emission and the lifetime spectra of the energy level $^5D_0$of europium have been studied. The mechanism, energy transfer efficiency from Tb^{3+} to Eu^{3+} and the influence of concentration of Eu^{3+} ions for photoluminescence properties of$CaMoO_4$ co–doped Eu^{3+} and Tb^{3+} nanophosphors have been analyzed.

Experimental

Synthesis nanophosphor

A series of nano-sized Eu^{3+}, Tb^{3+}co–doped $CaMoO_4$phosphors were synthesized by hydrothermal methodform$Ca_{0.99-y}Tb_{0.01}MoO_4$:$yEu^{3+}$(y = 0.01–0.10), using of some chemicals:$Ca(NO_3)_2.4H_2O$ (> 99%),$Na_2MoO_4.2H_2O$ (> 99.5%), Eu_2O_3 (99.99%), Tb_2O_3 (99.99%), HNO_3 (65%)and absolute ethanol (d = 0.790 $g.cm^{-3}$) were purchased from Merck. $Eu(NO_3)_3$and$Tb(NO_3)_3$solutions was obtained by dissolving $Eu_2O_3$and Tb_2O_3diluted in HNO_3 solution, heating at 60 °C on a magnetic stirrer for 30 min.

The synthesis of $Ca_{0.99-y}Tb_{0.01}MoO_4$:$yEu^{3+}$nanoluminescents are carried out according to the steps described in the diagram in Figure 1.

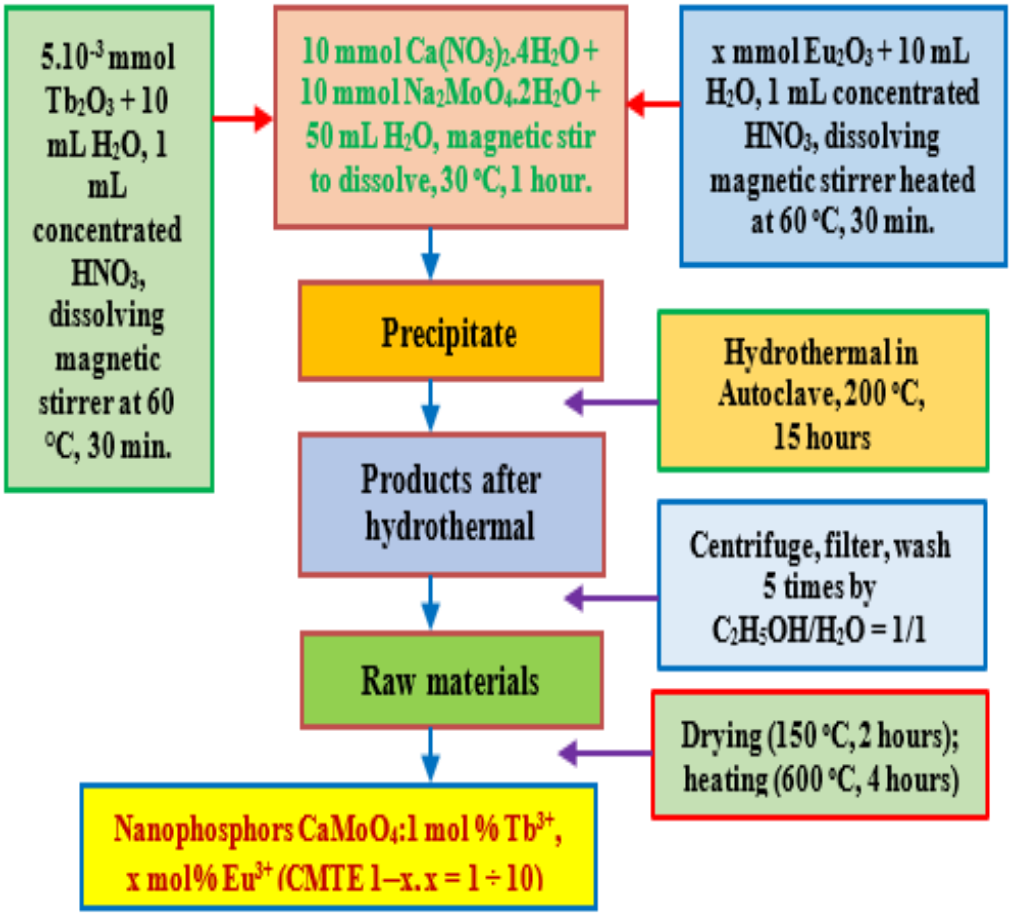

Figure 1:- Fabrication process of $Ca_{0.99-y}Tb_{0.01}MoO_4$:$yEu^{3+}$ (CMTE 1–x) nanophosphors annealed at 600 °C.

Instrumentation

Powder XRD measurement was done on a (D2 Phaser, Bruker, Germany) machine equipped with a CuKα radiation (λ = 1.54056 Å, 40 kV, 20 mA) in a 2θ scanning mode with a step size of 0.02° andacquisition speed of 4°/min. Raman measurement was acquiredusing a (XPLORA PLUS–Horiba) machine equipped with an argon laser(532 nm) in the range of 100–1000 cm^{-1}. The morphologicalcharacterization was carried out using a JEOL JSM–7600F fieldemission scanning electron microscopy (FE–SEM) (USA) operating under voltage 5KV.A spectrophotometer UV–Visible/NIR (Hitachi UH4150) were used to recordthe diffuse reflectance spectra (DRS) at 1 nm intervals and scan speed of 1200 nm/min from 240 to 2600 nm. The EDS system (Hitachi TM4000Plus) is used for analysis

elemental mapping. The measurements of photoluminescence excitation (PLE) and photoluminescence (PL) emission, and lifetime measurements were carried out using NANOLOG spectrophotometer (Horiba, USA) equipped with a 450 W Xe arc lamp and a dual excitation monochromator wwith divergence gap is 0.2 nm in size.

Results:-

XRD characters

Fig. 2 shows the XRD patterns of Tb^{3+} (1 mol%) and Eu^{3+} (1–10 mol%) co–doped $CaMoO_4$(denoted as CMTE 1–x) nanophosphors. All the X–ray diffraction peakswere observed at angles 2θ = ~ 18.18°, 28.64°, 30.77°, 33.77°,38.45°,46.60°, 48.77°, 53.59°, 57.55° and 59.04° corresponding to planes of the samples at (101), (112), (004), (200), (211), (204), (220), (116), (312) and(224)respectively. All the observed diffraction peaks are found to match with the tetragonal phase of $CaMoO_4$:(1–7%)Eu [10]and can be indexed with standard JCPDS card No. 29–0351[1–9, 11].Table 1 shows that the average particle size (D)was estimated from Scherrer's equation and was found to be inthe range 41.54–62.45 nm.

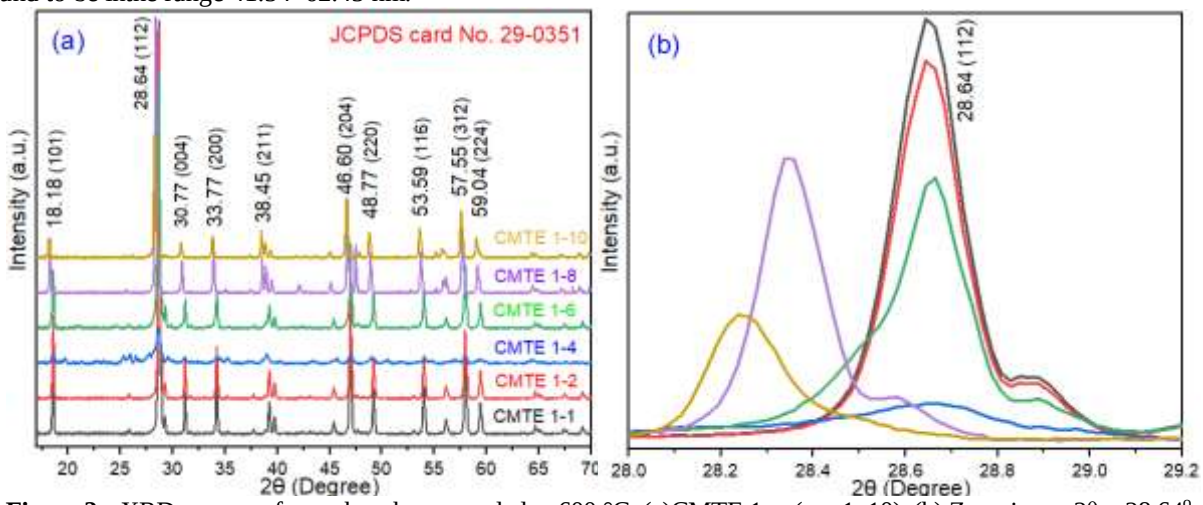

Figure 2:- XRD patternsofnanophosphorsannealed at 600 °C: (a)CMTE 1–x (x = 1–10), (b) Zooming at 2θ ≈ 28.64°.

Table 1:- Scherre's fomula for estimated crystal size (D) of CMTE 1–x at 2θ ≈ 28.64°.

Nanophosphor	CMTE**1**–**1**	CMTE**1**–2	CMTE**1**–**4**	CMTE**1**–**6**	CMTE**1**–**8**	CMTE**1**–10
FWHM (°)	0.12641	0.18946	0.14401	0.19005	0.15013	0.17844
D (nm)	62.45	41.67	54.82	41.54	52.58	44.24

When Tb/Eu is co–doped into the host lattice, it does not affect the crystal structure of the material and the sharp diffraction peaks prove that the CMTE sample has high purity and good crystallinity (Fig. 2a). The results showed that the Eu^{3+} (1.066 Å) and Tb^{3+} (1.027 Å) ions replaced the position of the Ca^{2+} ion (1.040 Å), which has a similar radius [2], but did not replace the position of the Mo^{6+} ion (0.410 Å), because its radius is much smaller. In other words, Tb^{3+} and Eu^{3+} ions easily penetrate the host lattice, creating crystals with few defects and strong luminescence.

Raman analysis

The micro–Raman spectra of the $Ca_{0.99-y}Tb_{0.01}MoO_4$:$yEu^{3+}$ phosphors in the range of 100 to 1000 cm^{-1} are presented in Fig. 3. The disordering of local symmetry can be probed with help of Raman scattering technique. There are 26 different vibration modes in the tetragonal structure $CaMoO_4$ crystal as obtained by the irreducible representation and they are described as follows:$\Gamma = {}^3A_g + {}^5A_u + {}^5B_g + {}^3B_u + {}^5E_g + {}^5E_u$, where: ${}^4A_u$ and ${}^4E_u$ are infrared and (${}^3A_g$, ${}^5B_g$ and ${}^5E_g$) are Raman-active; ^{3}Bu vibrations are silent modes; ${}^1A_u$ mode and ${}^1E_u$ mode are acoustic vibrations.

Result show that only have 9 vibration modes observed. The small change in polarizability will result in less intense peaks, the highly intense bands may hide some peaks, or the overlapping of bands may cause some peaks to unseen in the spectra. In thecase of $CaMoO_4$ nanophosphor, the modes observed at 119, 128.34, 160.29, 220.68, 293.21, 340.19 and 380.70 cm^{-1} are attributed to O–Mo–O vibrations. The peak at725.41 $cm^{-1}$is due to MoO_4 torsional modes. The peak found at 819.71 cm^{-1} isassigned as Mo–O_4 torsional mode. The mode at 879.05 cm^{-1} forms due toMo–O symmetric stretching vibrations. The substitution of Eu^{3+} and Tb^{3+}ions in $CaMoO_4$ give raise to the shifting of the peaks corresponding to theabove discussed modes and are shown in Table 2. A reasonableshift in the

wavenumber of all the modes has been observed when Eu^{3+}, Dy^{3+}ions are substituted at $CaMoO_4$ lattice. The aliovalent substitution of Eu^{3+}, Tb^{3+}ions for Ca^{2+} ions gives raise to the formation of oxygen vacancies inorder to preserve electron neutrality. Also, the entering of smaller Eu^{3+}, Tb^{3+}ions in Ca^{2+} sites causes the tilting of MoO_4tetrahedralresulting in thedistortion of local crystal structure symmetry. Presence of dopant ionsand oxygen vacancies in the system influence the band vibrations andhence modify the Raman modes. A further change in these vibrationalmodes is observed when Eu^{3+}, Tb^{3+} ions are substituted. This is because thesubstitution of Eu^{3+}, Tb^{3+}ions still enhances the oxygen vacancies and local structure distortion. But small shifts alone are foundin the vibrational modeswhen the concentration of Eu^{3+}, Tb^{3+} ions in $Ca_{0.99-y}Tb_{0.01}MoO_4$:$yEu^{3+}$ phosphor is altered [6]. The Raman scatteringvibrational modes of CMTE 1–x materials are in good agreement with $CaMoO_4$:(1–7%)Eu nanoluminescences, which have been studied and described previously [10].

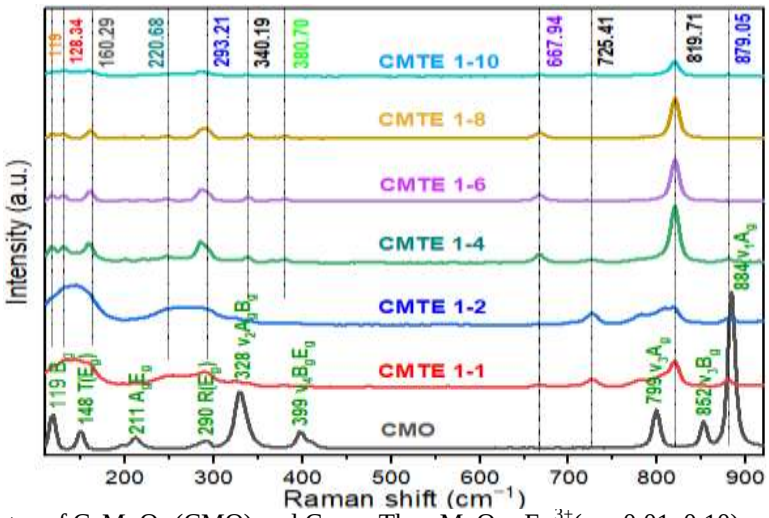

Figure 3:-Raman spectra of $CaMoO_4$ (CMO) and $Ca_{0.99-y}Tb_{0.01}MoO_4$:$yEu^{3+}$(y = 0.01–0.10) nanophosphorsannealed at 600 °C.

Table 2:- Assignments of Raman modes of $Ca_{0.99-y}Tb_{0.01}MoO_4$:$yEu^{3+}$ nanophosphors.

$CaMoO_4$(cm^{-1})	$CaMoO_4$:(1–7%)Eu(cm^{-1})[10]	$Ca_{0.99-y}Tb_{0.01}MoO_4$:$yEu^{3+}$, y = 0.01–0.10 ($cm^{-1}$)	Type of vibrations
119	115	128.34	T(B_g), $CaMoO_4$ lattice mode
148	140	160.29	T(E_g), O–Mo–O bending mode
211	205	220.68	(A_gE_g), O–Mo–O bending mode
290	267	293.21	R(E_g), O–Mo–O bending mode
328	320	340.19	ν_2(A_gB_g), O–Mo–O bending mode
399	390	380.70	ν_4(B_g) and ν_4(E_g), O–Mo–O bending mode
799	790	819.71	ν_3(E_g), Mo–O_4 torsional mode
852−884	845−879	879.05	ν_3(B_g), Mo–O_4 torsional mode and ν_1(A_g), Mo–O symmetric stretching

Morphology, composition and distribution of elements in the CMTE materials.

The FE–SEMand TEM observation (Fig. 4a–4d) shows the fabricated CMTE 1–x (x = 2, 6). The morphologies of samples with different doping concentrations are similar. The particle sizes are about 15–20 nm and uniformly distributed.

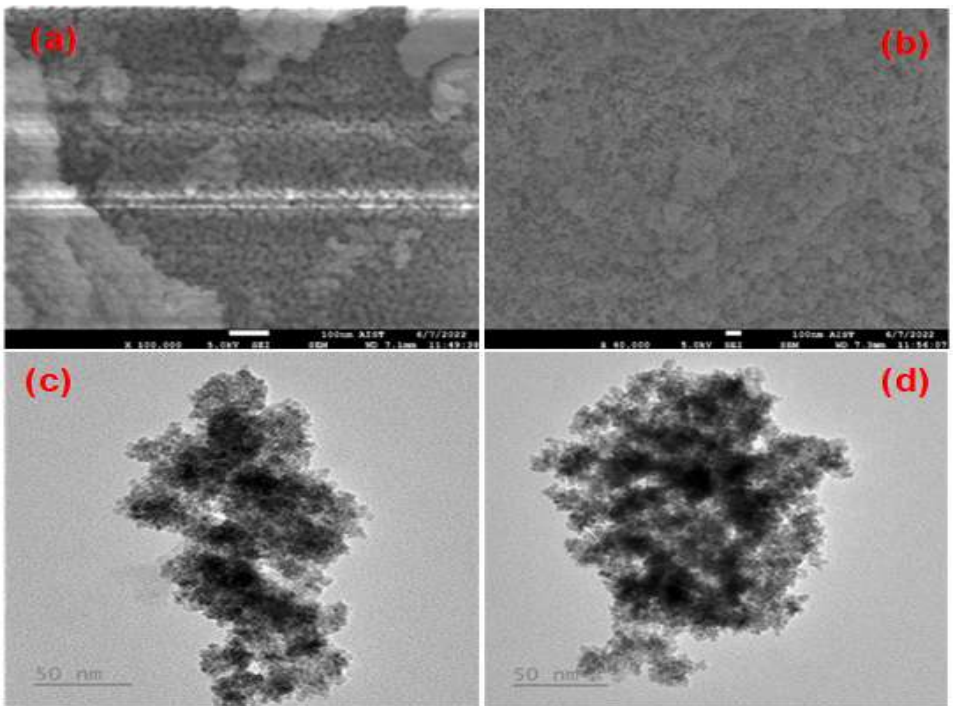

Figure 4:- FE-SEM images of nanophosphors: (a)CMTE 1–2; (b) CMTE 1–6 andTEM images of nanophosphors: (c) CMTE 1–2; (d) CMTE 1–6.

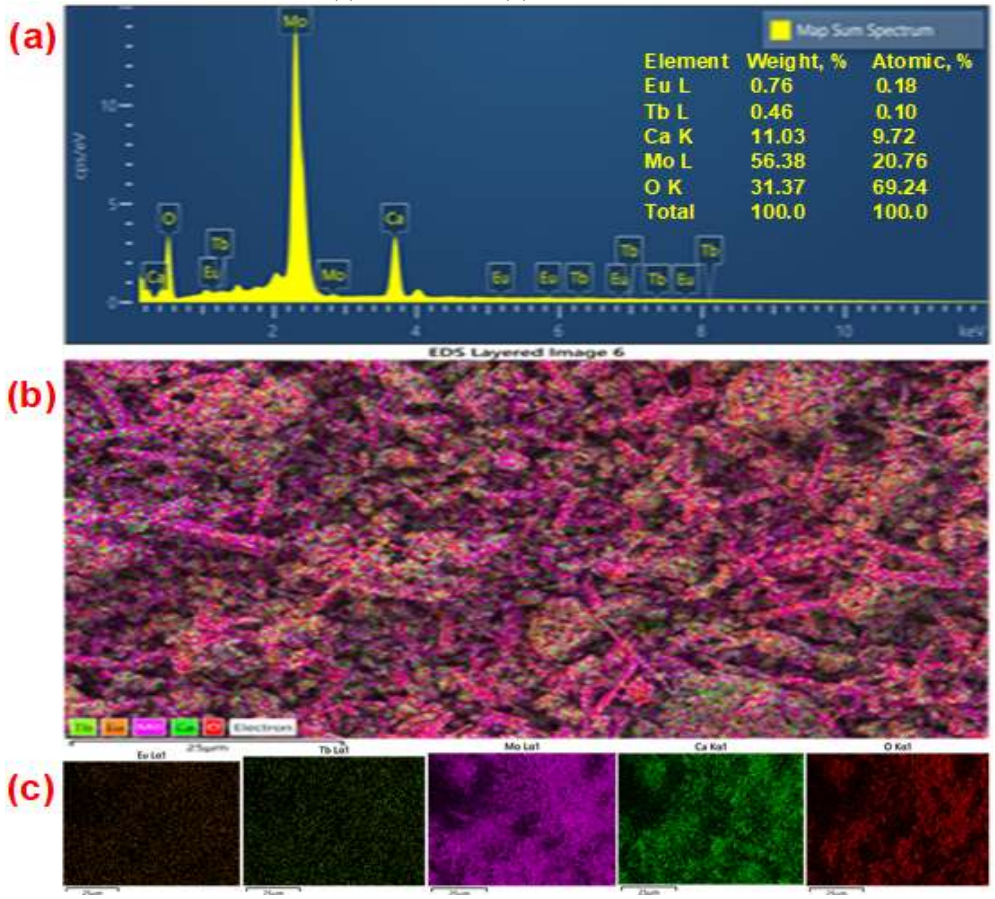

Figure 5:- The EDSof CMTE 1–1: (a) Elementimaging; (b) Mapping imaging; (c) Mapped color of Eu, Tb, Mo, Ca, O.

The EDS spectra of $Ca_{0.98}Tb_{0.01}MoO_4$:0.01Eunanophosphor shown in Fig. 5 confirms the presence of the elements asEu, Tb, Ca, Mo and O in the sample, which has both total weight % and total atomic % are 100 %, demonstrating the high purity of CMTE materials.The quantitative EDS analysis of the phosphor suggests that the obtained concentrations of the elements are close to the theoretical stoichiometry (Inset of Fig. 5a). Figure 5b show the X–ray dot mapping images of $Ca_{0.98}Tb_{0.01}MoO_4$:0.01Eu nanophosphor, results showed uniformly distribution of europium, tecbium, molybdenum, calcium and oxygen for all host matrix, which suggested that Eu^{3+} and Tb^{3+} co–doped of $CaMoO_4$ occurred homogenously.

Reflectance spectra and band gap

The diffuse reflectance spectra curve and the Kubelka-Munk energy curve of $Ca_{0.99-y}Tb_{0.01}MoO_4$:$yEu^{3+}$ (y = 0.01; 0.02; 0.04; 0.08) nanophosphors are shown in Fig. 6. The absorption band in the region 200–300 nm is found because of the collective effect of ligand–metal charge transfer transitions in Mo–O, Eu–Oand Tb–O groups. Small absorption peaks at 312–360 nmcorrespond to the intra f→f transitions of Eu^{3+} and Tb^{3+} ions.

The absorption wavelength shifts of the $Ca_{0.99-y}Tb_{0.01}MoO_4$:$yEu^{3+}$are determined about 408–431 nm, so the phosphors is absorbed in the visible light region. The E_g of $Ca_{0.99-y}Tb_{0.01}MoO_4$:$yEu^{3+}$is identified using Kubelka–Munk method and Tauc's equation as being about 2.8750–3.0417 eV, which is much lower than previous studies [2, 3,4,7]. The reflectancespectra demonstrate the probable excitation of these phosphors by radiations in the visible light region. Herein, the observed photoluminescence is due to the intra4f electronic transitions within the activator Eu^{3+}, Tb^{3+} ions and not due to theband gap absorption of the materials. These transitions occur within theband gap of the materials.

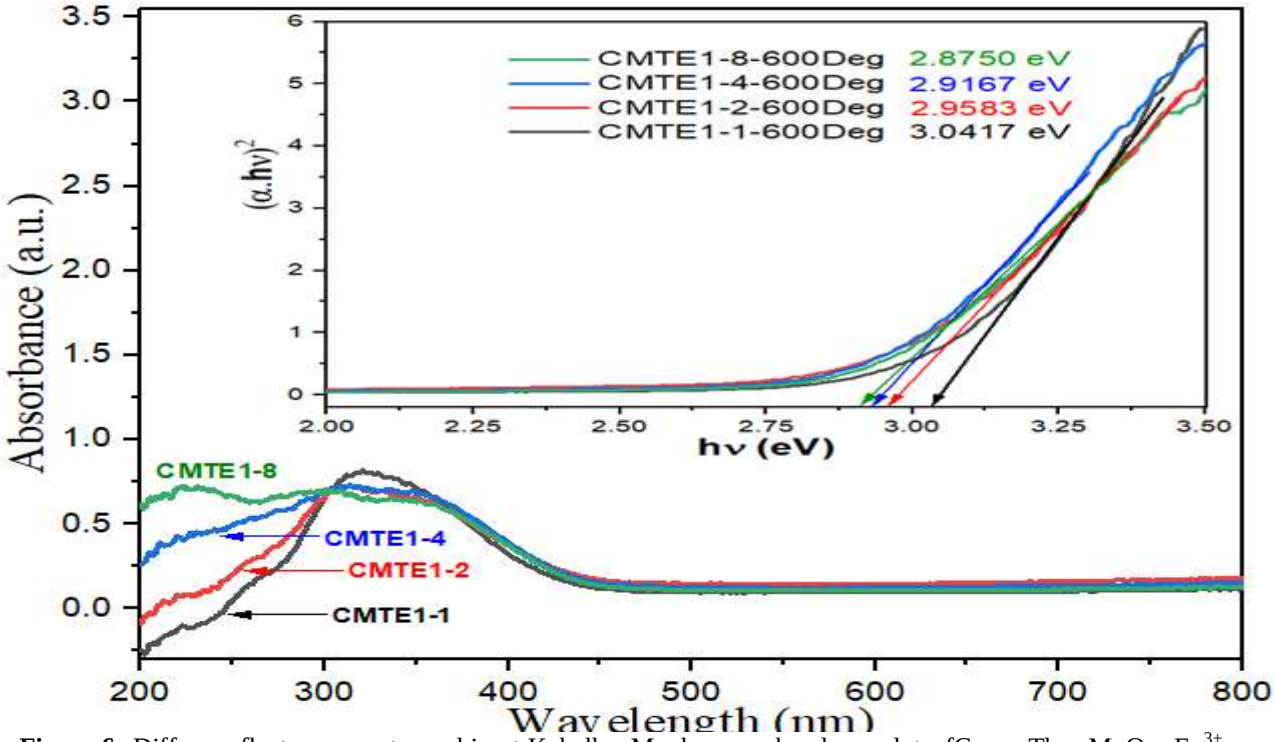

Figure 6:-Diffuse reflectance spectra and inset Kubelka–Munk versus band gap plotsof$Ca_{0.99-y}Tb_{0.01}MoO_4$:$yEu^{3+}$ nanophosphors.

PLE and PL of the CMTE samples

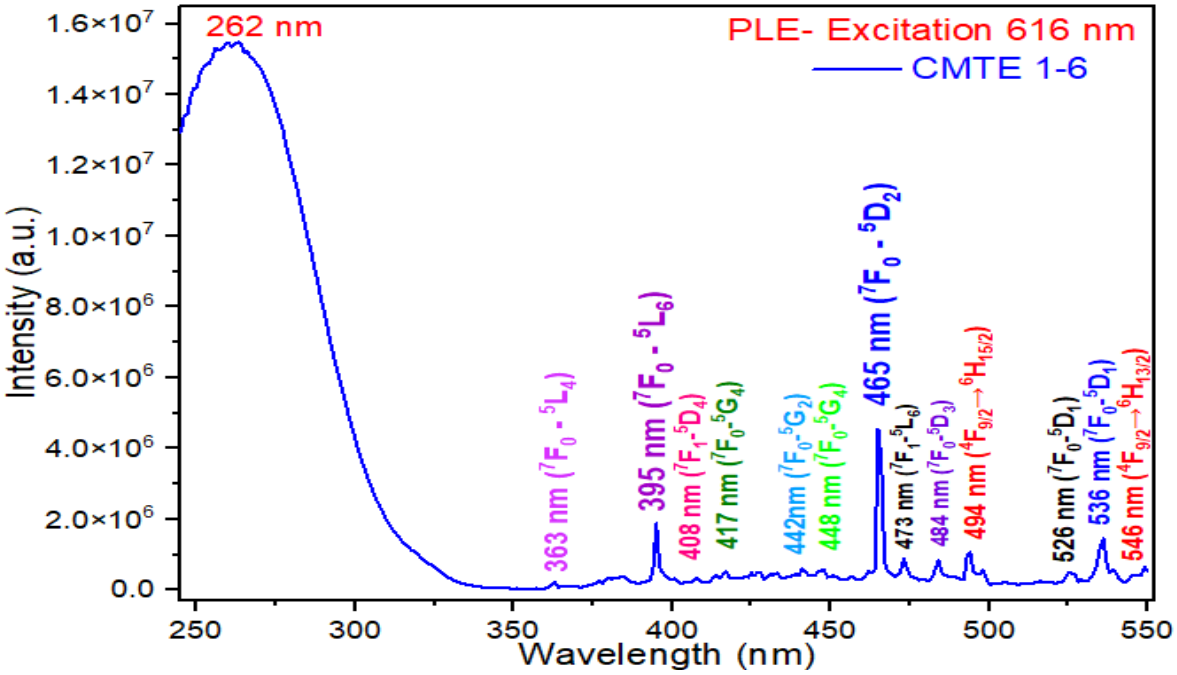

Figure 7:- PLE spectrum of $Ca_{0.93}Tb_{0.01}MoO_4$:0.06Eu (CMTE 1–6).

The excitation spectrum of the typical $Ca_{0.93}Tb_{0.01}MoO_4$:0.06Eu (Fig. 7) consists of characteristic 4f→4f transition peaks of Eu^{3+} and Tb^{3+} ions. At about 262 nm, which is charge transfer band (CTB), the excitation spectrum of nano–sized $Ca_{0.93}Tb_{0.01}MoO_4$:0.06Eu phosphor shows a broad band and several relatively weak were appeared between 350 and 550 nmdue to the charge transfer of the dominant MoO_4^{2-}group. As shown from Figure 7, the excitation spectrum is predominantly composed of two main parts: (1) The broad band in the range of 245–350 nm, which is ascribed to O^{2-}/Eu^{3+} and O^{2-}/Tb^{3+} charge transfer states (CTS), and Tb^{3+}/Eu^{3+} intervalence charge transfer, due to an electron transfer from 2p an (oxygen) orbital to an empty 4f shell of Eu^{3+}. (2) A different sharp line was found between 350 and 550 nm due to the f–f transition of Eu^{3+} and Tb^{3+} ions.

High extent of spectral splitting in this band is again endowed by the large crystalline field of the nano–sized CMTE samples. The observed excitation peaks are mainly due to the transitions from the 7F0 and 7F1 levels to the higher energy levels of the Eu^{3+} ion: $^7F_0 \rightarrow {}^5D_4$(363 nm); $^7F_1 \rightarrow {}^5D_4$(366 nm), $^7F_0 \rightarrow {}^5G_1$(377 nm), $^7F_0 \rightarrow {}^5G_2$(380 nm), $^7F_0 \rightarrow {}^5G_4$ (384 nm), $^7F_1 \rightarrow {}^5L_6$(408 nm), $^7F_0 \rightarrow {}^5D_3$(417 nm),$^7F_0 \rightarrow {}^5G_2$(442 nm), $^7F_0 \rightarrow {}^5G_4$(448 nm), $^7F_1 \rightarrow {}^5L_6$(473 nm),$^7F_0 \rightarrow {}^5D_3$ (484 nm),$^7F_0 \rightarrow {}^5D_1$(526 nm), and $^7F_0 \rightarrow {}^5D_1$(536 nm). The observed relatively weak peaks at 494, and 546 nm are assigned to electronic transitions of $^4F_{9/2} \rightarrow {}^6H_{15/2}$, and $^4F_{9/2} \rightarrow {}^6H_{13/2}$, respectively, which are originated from the 4f–4f transitions of Tb^{3+}. At 395 nm and 465 nm excitations, the intense sharp peaks were observed which consistent to $^7F_0 \rightarrow {}^5L_6$ and $^7F_0 \rightarrow {}^5D_2$transitions, have wavelengths consistent with the characteristic emission from near–UV/UV LEDs and blue LEDs, so the prepared $Ca_{0.99\text{-}y}Tb_{0.01}MoO_4$:$yEu^{3+}$phosphors greatly promises for potential practical applications of wLED and blue LEDs [2–10].

It is to be understood here that f–f transitions are forbidden and are absent in pure Tb_2O_3. As a result of orbital mixing when incorporated in a crystalline host, these transitions appear due to the relaxation of the LaPorte parity rule. Moreover, symmetry around Tb^{3+} ions has an important role in dictating its intensity and appearance. Intrinsic porous characteristics, high surface area, and defects of the nano–sized sample make it more distorted in nature, and hence, the local symmetry around Tb^{3+} in the nano–sized CMTE is low. Lower symmetry of Tb^{3+} in the nano–sized CMTE relaxes the selection rule, making the appearance of the intra–configurational f–f bands of Tb^{3+} ion in the excitation spectrum. On the other hand, in the case of the bulkCMTE sample, because of the reduced surface to volume ratio and enhanced compactness of the local symmetry around Tb^{3+}, high symmetry around Tb^{3+} ions makes the f–f selection rule more stringent and curtails the appearance of intra–configurational f–f bands of Tb^{3+} ion in the excitation spectrum of the bulk CMTE nanophosphors[2–10].

As shown from Figure 8, the room temperature PL emissionspectra of $Ca_{0.99-y}Tb_{0.01}MoO_4:yEu^{3+}$ nanophosphors were measured, in which the excitation wavelength was monitored at 395 nm. The emission spectra were composed of a series ofsharp emission lines, corresponding to transitions from the excited states $^5D_0$ to the ground state ^7F_j (j = 0, 1, 2, 3, 4). At about 596 nm, the emission of orange color was observed which is belongs to the magnetic dipole $^5D_0 \rightarrow {}^7F_1$ transition of Eu^{3+}, and the transition hardly varies with the crystal field strength $^5D_0 \rightarrow {}^7F_2$ transition of Eu^{3+}, which is very sensitive to the local environment around Eu^{3+} ions, which belongs to the electric dipole effects in which the red emissions were observed at 616 nm. In spite of this, it depends on the symmetry of the crystal field. Two strong peaks which were found at 596 and 616 nm emissions peaks, which are magnetic and electric dipole transitions of Eu^{3+} ions respectively, indicate that there are two Ca^{2+} positions in the $Ca_{0.99-y}Tb_{0.01}MoO_4:yEu^{3+}$ lattice. One position, Ca(I), is inversion symmetry and the other side, Ca(II), is noninversion symmetry. Other two emission peaks located at 655 and 702 nm are relatively weak, which is corresponding to the $^5D_0 \rightarrow {}^7F_3$ and $^5D_0 \rightarrow {}^7F_4$typical transitions of Eu^{3+} ions, respectively.

A fairly strong peak at 545 nm($^5D_4 \rightarrow {}^7F_5$), and emission peaks located at 489 nm, 592 nm, 613 nm, 652 nm, 695 nm are relatively weak, which is corresponding to the $^5D_4 \rightarrow {}^7F_j$(j = 6–1)typical transitions of Tb^{3+} ions, respectively, all of which are electric dipole transitions. From this result, it was shown that when doping Eu^{3+} and Tb^{3+} ions into $CaMoO_4$, there was efficient energy transfer from the matrix to the energy levels of $Eu^{3+}$and Tb^{3+}ions [4–9, 12–13].The strong luminescence of the electric dipole transitions show that $Eu^{3+}$and Tb^{3+}ions have replaced Ca^{2+} ions.

It can be seen from the figure 8 that there is not much change in the emission spectral features as a function Eu^{3+} ion concentration. However,emission intensity gradually increased when doping 1.0 to 4.0 mol% Eu^{3+} and then gradually decreased when the doping concentration of Eu^{3+} was greater than 4 mol%. This resulted from energy transfer from Tb^{3+} ions to Eu^{3+} ions, which caused concentration quenching of luminescence intensity.

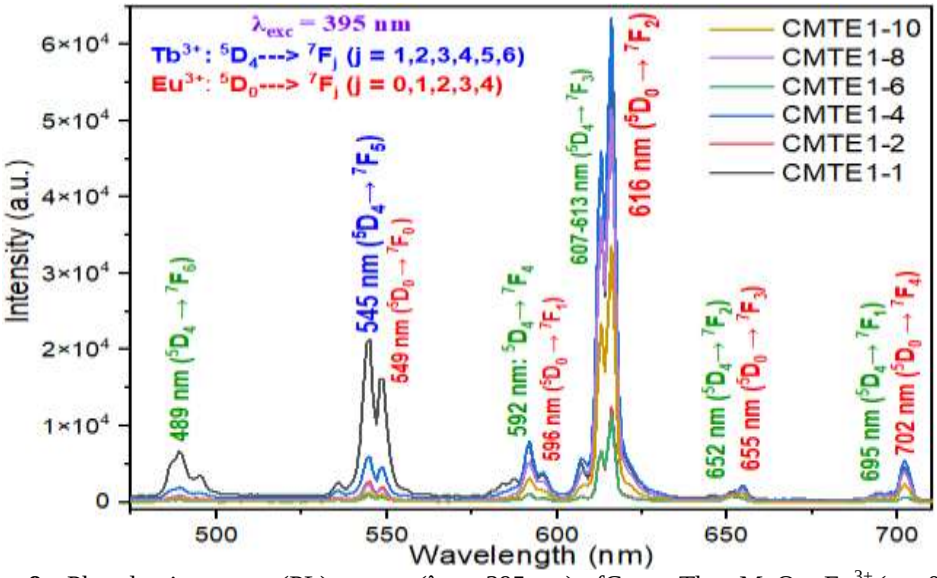

Figure 8:- Photoluminescence (PL) spectra (λ_{exc} =395 nm) of$Ca_{0.99-y}Tb_{0.01}MoO_4:yEu^{3+}$ (y = 0.01–0.10)nanophosphors annealed at 600 ^oC temperatures in air.

Table 3:- The ratio $I_{616\ nm}/(I_{545\ nm} + I_{616\ nm})$ of theCMTE 1–xnanophosphors.

Nanophosphor / Intensity (a.u.)	CMTE1–1	CMTE1–2	CMTE1–4	CMTE1–6	CMTE1–8	CMTE1–10
$I_{545\ nm}$ (a.u.)	21379	2722	5943	872	2238	1257
$I_{616\ nm}$(a.u.)	58479	12474	63486	11383	51511	33575
$I_{616\ nm}/(I_{545nm}+ I_{616\ nm})$	0.7323	0.8209	0.9144	0.9288	0.9584	0.9639

Table 3 show ratios of the emission intensity at 616 nm (red, $^5D_0 \rightarrow {}^7F_2$) to the sum of the intensities at 616 nm and 545 nm (green, $^5D_4 \rightarrow {}^7F_5$) in the Eu^{3+} and Tb^{3+} co–doped $CaMoO_4$nanophosphors.When x value increase, the emission intensities at 616 nm and 545 nm simultaneously increased and decreased, respectively. The ratio of the emission intensity at 616 nm to the sum of the intensities at 616 nmand 545 nm increased with increasing the x value from 1 to 10 mol% in the $CaMoO_4$:0.01Tb^{3+},xEu^{3+} nanophosphors.Thus, the red emission ($^5D_0 \rightarrow {}^7F_2$) of Eu^{3+} ion was enhanced in the presence of Tb^{3+}sensitizer ion in $CaMoO_4$:1%Tb^{3+},x%Eu^{3+} nanophosphors. Showing that there is effective energy transfer from Tb^{3+} to Eu^{3+} ions.

In addition, compared with the nano–size $CaMoO_4$ doped 5% Eu^{3+}, which has intensities ratio $I_{616\ nm}/(I_{545\ nm} + I_{616\ nm})$ was 0.9930 ≈ 1.0 [10] and higher than the nanoluminescents $CaMoO_4$ co–doped Eu^{3+} and Tb^{3+}, showing that the CMTE 1–x nanophosphors are colors tunable, the photoluminescent colors could be transferred from green to red easily with of different ratios of Eu^{3+} and Tb^{3+}.

The energy transfer mechanismfrom $Tb^{3+}$to Eu^{3+}

It is well known that energy transfer (ET) of phosphors can be produced by exchange interactions or electrical multipole interactions mainly between luminescent centers. These interactions depend on the critical distance $R_{Tb \rightarrow Eu}$ between the Tb^{3+} and Eu^{3+} ions. With 5–7 Å as the boundary, exchange interactions play a role when the critical distance not exceed about 5 Å, while electrical multipole interactions dominate if $R_{Tb \rightarrow Eu}$ is larger than 7 Å [8].

To have better understanding of concentration quenching mechanism the critical distance ($R_{Tb \rightarrow Eu}$) for the energy transfer has been calculatedfrom the geometrical factors of the host using the relation given byBlasse, according to formula (1) [4–8]:

$$R_{Tb \rightarrow Eu} = 2\left(\frac{3V}{4\pi X_c N}\right)^{\frac{1}{3}} \qquad (1)$$

where $R_{Tb \rightarrow Eu}$ is the critical distance between the dopant ion and quenching site, V is the volume of the unit cell, X_c is thetotal critical concentration of Eu^{3+} and Tb^{3+} ions, and N the number of crystallographic sites available for dopant or the activator ions in the unit cell. For $CaMoO_4$ host lattice V = 313.013 $Å^3$(a = b = 5.2300 Å, c = 11.4435 Å) [8], N = 4 (four formula units per one unit cell), and X_c = 0.02–0.11. Based on the values, the average distances of the donor–acceptor in the current situation are calculated to be 7.786–13.744 Å, which are larger than the critical value (5–7 Å). This result suggests that the energy transfer through the exchange interaction is impossible and the energy transfer from Tb^{3+} to Eu^{3+} ions in the CMTE 1–x phosphors is mainly by an electric multipole interaction.

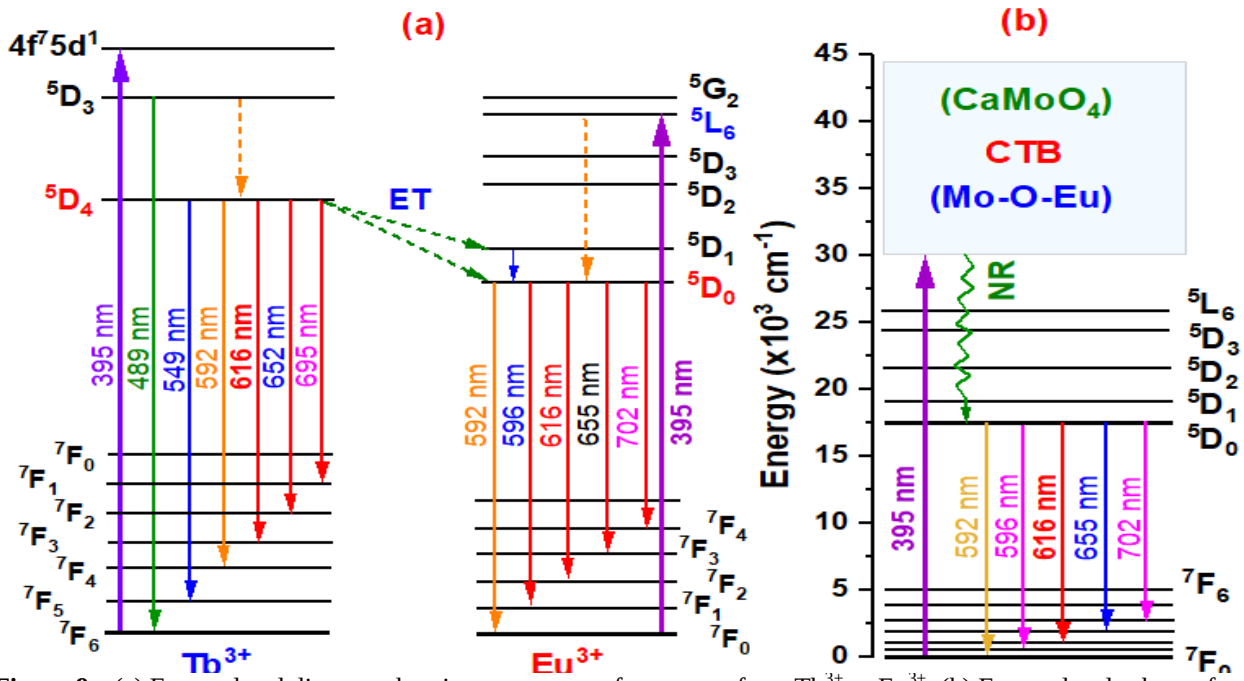

Figure 9:- (a) Energy level diagram showing energy transfer process from Tb^{3+} to Eu^{3+}; (b) Energy level scheme for the emission process in $Ca_{0.99-y}Tb_{0.01}MoO_4$:y$Eu^{3+}$nanophosphors.

The proposed path for the energy transfer to occur in co–doped glasses could be $^5D_4$ of Tb^{3+} to $^5D_0$ state of Eu^{3+} ions. This is shown in Fig. 9 where an excitation wavelength 395 nm raises Tb^{3+} ions to a higher energy state ($4f^75d^1$) which can relaxe to the $^5D_4$ state by emitting non–radiative energy which is than absorbed by Eu^{3+} ions in the ground state which are excited to higher energy states and then relaxes to $^5D_0$ state. Further they cascade non–radiatively to intermediate states $^5D_1$ and $^5D_0$ and therefore finally decay radiatively to $^7F_0$ ground state [8–9, 12–13].

CIE and CCT studies

Figure 10 shows the color coordinate diagram (CIE) and correlated color temperature (CCT) of CMTE 1–x (x = 1–10) materials calcined at 600 ^oC. The CIE and CCT color coordinate values of the samples are listed in table 4, demonstrating the luminescence of CMTE materials in the red region from (0.484; 0.428) to (0.606; 0.337) with CCT values large in the range 1142–2512 K, which values are equivalent to light on a clear day compared to common color temperature tables. These results are consistent with previous studies [5–6].

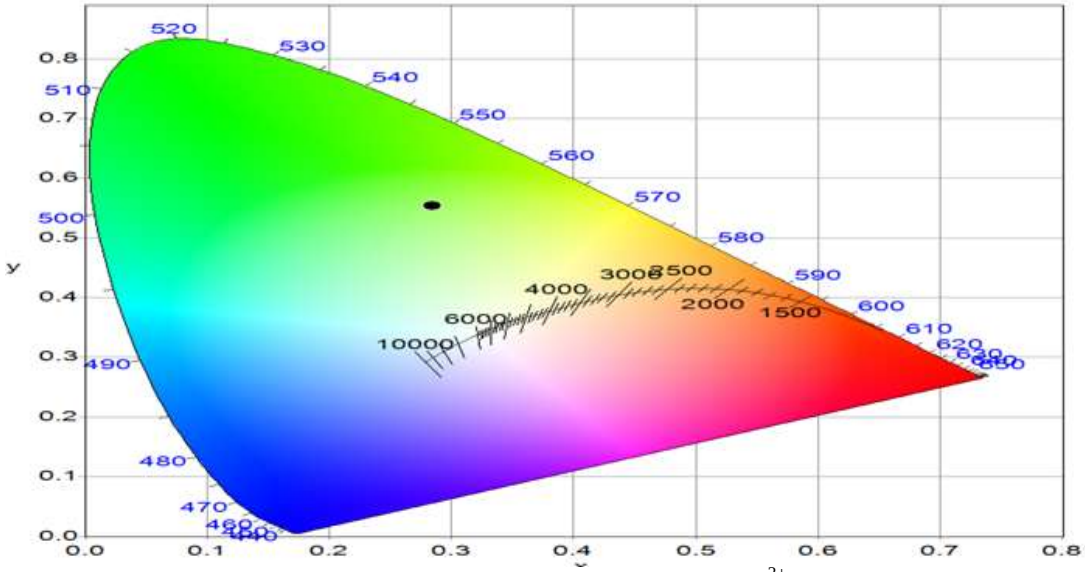

Figure 10:- CIE and CCT diagram of$Ca_{0.99-y}Tb_{0.01}MoO_4$:y$Eu^{3+}$ nanophosphors.

Table 4:- CIE and CCT values of $Ca_{0.99-y}Tb_{0.01}MoO_4:yEu^{3+}$nanophosphors.

Nanophosphor	CIE		CCT (K)
	xaxis	yaxis	
CMTE 1–0	0.285	0.554	N/A
CMTE 1–1	0.484	0.428	2512
CMTE1–2	0.528	0.373	1745
CMTE1–4	0.571	0.370	1465
CMTE1–6	0.606	0.337	1142
CMTE1–8	0.522	0.367	1748
CMTE1–10	0.552	0.356	1498

Fluorescencelifetime, energy transfer efficiency and concentration quenching mechanism

The decay profiles of the emission spectra of 1 mol% Tb^{3+} and y (from 0.01 to 0.06 mol%) Eu^{3+} co–doped $CaMoO_4$, are recorded at 395 nm excitation and 616 nm emission wavelength for the energy level $^5D_0$. The decay profiles are shown in Fig. 12. The decay curves were observed to have biexponential nature and further analyzed to understand the energy transfer behavior from Tb^{3+} ion to Eu^{3+} ion. The average value of lifetime (τ) was calculated as follows formula (2)and the values are presented in Fig. 11:

$$\tau = \frac{A_1 t_1^2 + A_2 t_2^2}{A_1 t_1 + A_1 t_2} \qquad (2)$$

Where t_1 and t_2 stands for fast and slow decay times respectively; A_1 and $A_2$are constants. The obtained τ values are 0.81165–1.19950 ms and the lifetime values were decreased as compared to singly doped 1 mol%Tb^{3+}(CMT1) such as (τ_{Tb}) is 2.87241 ms, which supported the previous non radiative energy transfer arguments and suggested that Tb^{3+} is acting as sensitizer while Eu^{3+} is acting as activator in this matrix. The trend of observed decay values is also due to mix rare earth ion effect since here concentration of both the RE^{3+} ions are varied [8].

The energy transfer rate ($A_{da(Tb\rightarrow Eu)}$) from $Tb^{3+}$to $Eu^{3+}$is also calculated by the following equation(3) and the efficiency of energy transfer ($\eta_{Tb\rightarrow Eu}$) from Tb^{3+} to Eu^{3+} are calculated by the equation (4), and the efficiency of energy transfer ($\eta_{CMO\rightarrow Eu}$) from CMO to Eu^{3+} are calculated by the equation (5). The τ_{Tb} and τ in the above relation are the corresponding lifetime decays of Eu^{3+} ions in single–doped and co–doped Eu^{3+}/Tb^{3+}respectively [8].

$$A_{da(Tb\rightarrow Eu)} = \frac{1}{\tau} - \frac{1}{\tau_{Tb}} \quad (3) \qquad \eta_{Tb\rightarrow Eu} = 1 - \frac{\tau}{\tau_{Tb}} \quad (4) \qquad \eta_{CMO\rightarrow Eu} = 1 - \frac{\tau_{CMO}}{\tau} \quad (5)$$

The $A_{da(Tb\rightarrow Eu)}$, $\eta_{Tb\rightarrow Eu}$ and $\eta_{CMO\rightarrow Eu}$ of CMTE 1–x nanophosphors arepresented in table 5.

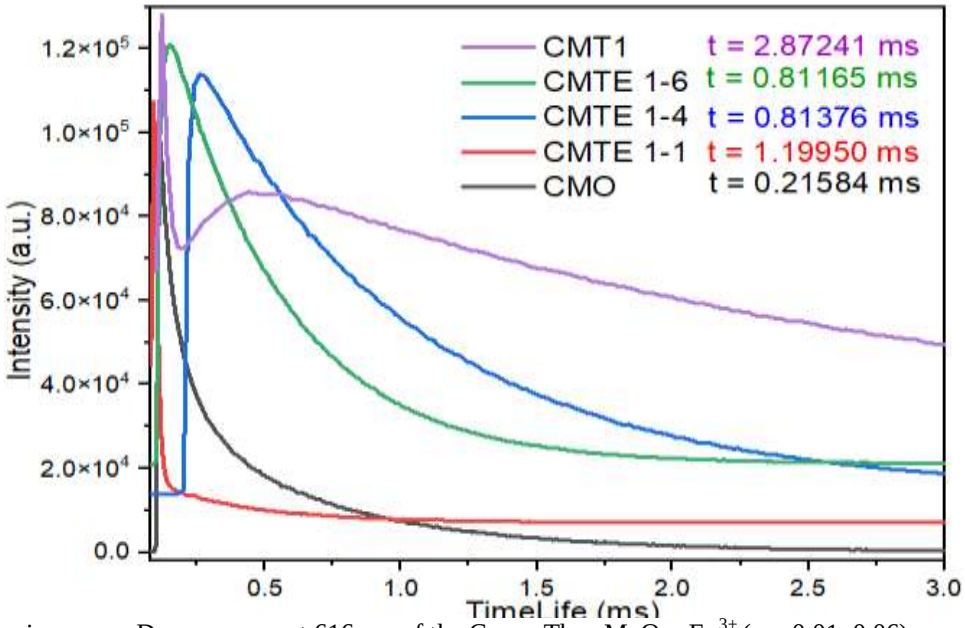

Figure 11:- Luminescence Decay curves at 616 nm of the $Ca_{0.99-y}Tb_{0.01}MoO_4$:y$Eu^{3+}$ (y = 0.01–0.06)nanophosphors annealed at 600 ^oC under the excitation wavelength of 395 nm.

Table 5:- Average lifetime, energy transfer rate, efficiency, and average distance of CMTE 1–x nanophosphors.

Nanophosphor	τ	$\eta_{Tb\rightarrow Eu}$ (%)	$\eta_{CMO\rightarrow Eu}$ (%)	$A_{da(Tb\rightarrow Eu)}$ (s^{-1})	$R_{Tb\rightarrow Eu}$ (Å)
CMT1	2.87241 (τ_{Tb})	-	-	-	-
CMTE 1–1	1.1995	0.5824	0.8201	485.54	7.7861
CMTE 1–4	0.81376	0.7167	0.7348	880.72	10.5673
CMTE 1–6	0.81165	0.7174	0.7341	883.92	11.8215
CMO	0.21584	-	-	-	-

Table 5 shows, that the lifetime of nanophosphors gradually decreased with increased Eu^{3+} doped in, this is because the electrons have more opportunities to move from a higher energy level to a lower energy level and this can cause the time the electrons spend to stay at the energy level to decrease. The possible energy transfer channels attributed to the going out of $^5D_4$fluorescence of Tb^{3+} by $Eu^{3+}$are shown in Fig. 9a. The energy transfer from Tb^{3+}ionto Eu^{3+}ion is very efficient because they have large emission spectra overlapping each other.Addition, the increasing of Eu^{3+}co–doped, both $\eta_{Tb\rightarrow Eu}$ and $A_{da(Tb\rightarrow Eu)}$ are increased.

The concentration dependent luminescence intensities are fitted to Dexter's energy transfer formula for multipolar interaction and Reisfeld's approximation by equation (6) below:

$$\log(I/(0.01+y)) = C - (\theta/3)*\log(0.01+y) \quad (6)$$

where I is emission intensity, (0.01+y) is the total concentration of Tb^{3+} and Eu^{3+}, C and θ are fitting constants. As per the above formalism, the value of the fitting constant θ is in the increasing order for exchange coupling, electric dipole–dipole, dipole–quadrupole and quadrupole–quadrupole interactions and the values are 3, 6, 8 and 10, respectively [4, 6–8]. The intensity data is fitted to Equ. (6) and given in Fig. 12. From the slope, the θ value is ~6.004 which is close to 6 showing that the dominant concentration quenching mechanism of Tb^{3+} and Eu^{3+} in $CaMoO_4$is the non–radiative dipole–dipole interaction [8].

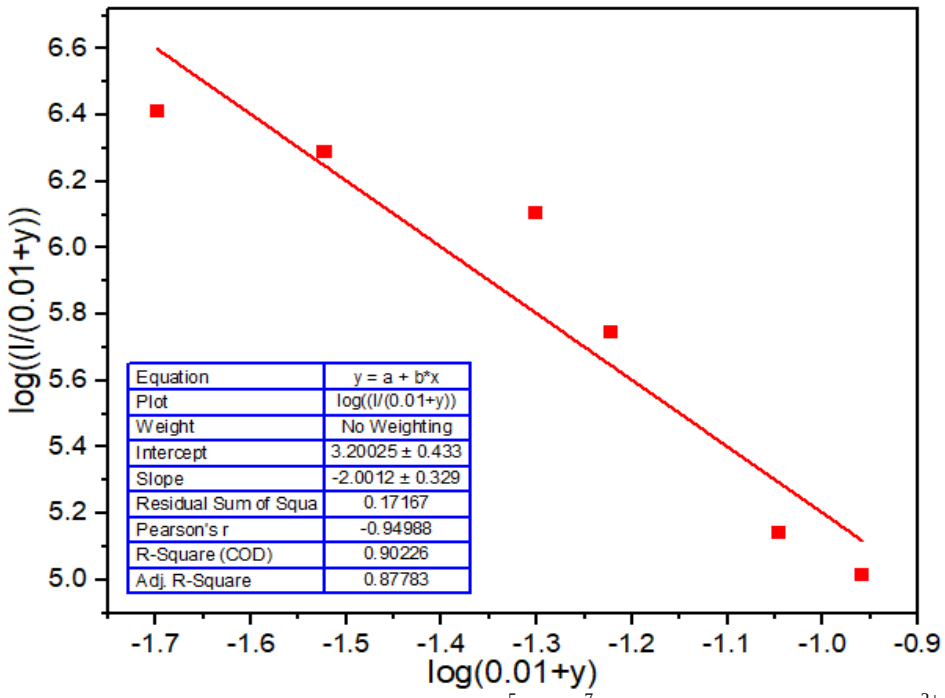

Figure 12:- log(I/(0.01+y)) vs log(0.01+y) plot of the $^5D_0 \rightarrow {}^7F_2$ transition intensity (I) of Eu^{3+} ions in $Ca_{0.97-y}Tb_{0.01}MoO_4:yEu^{3+}$(y = 0.01–0.10) and the line and co–doping concentration (0.01+y) is fit with equation (6).

Conclusions:-

The influence of co–doped Tb^{3+} ion in enhancing the photoluminescence properties of $CaMoO_4:Eu^{3+}$was studied by examining characteristics of nanophosphors using modern analysis methods. The $Ca_{0.99-y}Tb_{0.01}MoO_4:yEu^{3+}$materials as well as red nanophosphors, were successfullyprepared viahydrothermaltechnique.

The nanostructure analysis and surface morphology were studiedusingscanning and transmission electron microscopy spectroscopy techniques. Eu^{3+} and Tb^{3+} ions occupied the position of Ca^{2+} ions, were verified by XRD pattern, Raman scattering and EDSelemental/mapping studies.The Raman spectra analysis confirmed that the substitution of rare earth ions altered the local crystal structure symmetry.The photoluminescence (PL) spectra of $Ca_{0.99-y}Tb_{0.01}MoO_4:yEu^{3+}$ nanophosphors show emission peak at 616 nm ($^5D_0 \rightarrow {}^7F_2$) correspondingto the red region from (0.484; 0.428) to (0.606; 0.337)of CIE. The co–doped of Tb^{3+} ions brought about 5.6 timesenhancement of luminescence intensity and the luminescence lifetime value calculated about0.81165–1.19950 ms.The increasing of Eu^{3+} co–doped, both the energy transfer rate and the efficiency of energy transfer from Tb^{3+} ions to Eu^{3+} ions is are increased. This research showed that co–doped $CaMoO_4$:1%Tb^{3+},x%Eu^{3+}nanophosphorshave a potential for application as a red–emitting powder for warm white LEDs.

Author Contributions:
N.C.M has contributed to Sample synthesis, Sample processing, Data analysis, Intellectual content design, Result interpretation and Writing–original draft preparation. Collection of samples, Interpreting resultdata curation, Software and Conceptualization by H.P.V, M.A.P. Writing–review and editing by N.C.M, H.P.V. All authors have drafted, read and agreed to the published version of the manuscript.

Supervision:
N.C.M.

Acknowledgments:-

This research is funded by Thai Nguyen University under grant number ĐH2022-TN04-01.

Ethical approval and consent:
Not applicable.

References:-

[1].A. Khanna, P.S. Dutta. Narrow spectral emission $CaMoO_4$: Eu^{3+}, Dy^{3+}, Tb^{3+} phosphor crystals for white light emitting diodes. Journal of Solid State Chemistry,vol.198 (2013): 93–100.http://dx.doi.org/10.1016/j.jssc.2012.08.060.

[2].Akta Verma, S.K. Sharma.Rare-earth doped/co-doped $CaMoO_4$ phosphors: A candidate for solar spectrum conversion.Solid State Sciences 96 (2019) 105945: 1–10, 2019. https://doi.org/10.1016/j.solidstatesciences.2019.105945.

[3]. Anees A. Ansari, A.K. Parchur, M. Alam, Abdallah Azzeer. Structural and photoluminescence properties of Tb-doped $CaMoO_4$ nanoparticles with sequential surface coatings. Materials Chemistry and Physics147 (2014): 715–721,2014. http://dx.doi.org/10.1016/j.matchemphys.2014.06.011.

[4]. Yongqing Zhai, Xin Zhao, Chang Liu, Pengfei Song, Xuemeng Jing, Ying Han, Jing Wang. $CaMoO_4$:Dy^{3+}, Eu^{3+} phosphors: microwave synthesis, characterization, tunable luminescence properties and energy transfer mechanism.Optik164 (2018): 433–442.https://doi.org/10.1016/j.ijleo.2018.03.049.

[5].Shidong Li, Qingyu Meng, Shuchen Lü, Wenjun Sun. Study on optical temperature sensing properties of Tb^{3+}, Eu^{3+} co-doped $CaMoO_4$ phosphor. Journal of Luminescence 200 (2018): 103–110. https://doi.org/10.1016/j.jlumin.2018.04.009.

[6]. Hyun-Woo Lee, Young-Duk Huh. Preparation of transparent suspensions of tunable-emission $CaMoO_4$:(1-x)Eu^{3+},(x)Tb^{3+} nanophosphors.Optical Materials111 (2021)110594: 1–7. https://doi.org/10.1016/j.optmat.2020.110594.

[7].R. L. Tranquilin, L. X. Lovisa, C. R. R. Almeida, C. A. Paskocimas, M. S. Li, M. C. Oliveira, L. Gracia, J. Andres, E. Longo, F. V. Motta, and M. R. D. Bomio. Understanding the White-Emitting $CaMoO_4$ co-doped Eu^{3+}, Tb^{3+},and Tm^{3+} Phosphor through Experiment and Computation.J. Phys. Chem. C 2019, 123: 18536–18550.DOI: 10.1021/acs.jpcc.9b04123.

[8]. XIONG Jianhui, MENG Qingyu, SUN Wenjun. Luminescent properties and energy transfer mechanism from Tb^{3+} to Eu^{3+} in $CaMoO_4$:Tb^{3+},Eu^{3+} phosphors.Journal of rare earths, Vol. 34, No. 3: 251–258, 2016.DOI: 10.1016/S1002-0721(16)60022-4.

[9]. Jiaming Deng, Zihao Wang, Weiping Zhou, Mingyuan Yu, Jiangen Min, Xunliang Jiang, Ziyan Xue, Chunlin Ma, Zhenzhi Cheng, Guangsheng Luo. Energy transfer of Tb^{3+}→Eu^{3+} in $Ca_2Al_2SiO_7$ phosphors with multicolor tunable and optical temperature sensing properties. Ceramics International49 (2023):14478–14486.https://doi.org/10.1016/j.ceramint.2023.01.036.

[10]. N.C. Manh, L.T.H. Nguyen, T.M. Xuan, H.D. Tra, T.T. Anh Duong, L.T.T.Nguyen, H. Van Pham, M.N. Ha, V.H. Nguyen, H.D. Chau, T.K. Ngan Tran. Temperature affects on the photoluminescence and Judd-Ofelt intensity parameters of $CaMoO_4$:Eu^{3+} nanophosphor. Journal of Luminescence(2023), 119776: 1–9. Doi: https://doi.org/10.1016/j.jlumin.2023.119776.

[11]. Zhi-Jun Zhang, Hao-Hong Chen, Xin-Xin Yang, Jing-Tai Zhao. Preparation and luminescent properties of Eu^{3+} and Tb^{3+} ions in the host of $CaMoO_4$. Materials Science and Engineering B 145 (2007): 34–40. Doi:10.1016/j.mseb.2007.09.091.

[12]. D. Rajesh, K. Brahmachary, Y.C. Ratnakaram, N. Kiran, A.P. Baker, G.G. Wang. Energy transfer based emission analysis of Dy^{3+}/Eu^{3+} co-doped ZANP glasses for white LED applications. J. Alloys Compd. 646 (2015): 1096–1103. https://doi.org/10.1016/j.jallcom.2015.05.138.

[13]. B. Devakumar, P. Halappa, C. Shivakumara. Dy^{3+}/Eu^{3+} co-doped $CsGd(MoO_4)_2$ phosphor with tunable photoluminescence properties for near-UV WLEDs applications. Dyes Pigments 137 (2017): 244–255. http://dx.doi.org/10.1016/j.dyepig.2016.10.016.